Journal Name

ARTICLE

Ultrahigh iodine adsorption in porous organic frameworks

Cuiying Pei,[a] Teng Ben,*[b] Shixian Xu,[a] and Shilun Qiu*[a]

We present two porous organic frameworks (POFs), PAF-1 and JUC-Z2, with ultrahigh iodine capture capacity. The iodine vapor uptake of PAF-1 and JUC-Z2 were 1.86 g g^{-1} and 1.44 g g^{-1} respectively at 298 K / 40 Pa, which is extremely high for such low pressure sorption condition. In addition, PAF-1 and JUC-Z2 could adsorb iodine over water with the selectivity of 5.1 and 6.5 respectively. The isosteric enthalpy at zero surface coverage, calculated by a virial equation with the iodine vapor sorption isotherms at 298 K and 313 K of JUC-Z2, reached -51.1 kJ mol^{-1}, which was much higher than the coverage of PAF-1 (-14.9 kJ mol^{-1}). Raman measurement confirmed the polyiodide to be I_5^- in POFs. Furthermore, solvents with different polarities, such as n-hexane, chloroform, and methanol, were chosen to conduct iodine binding measurements on PAF-1 and JUC-Z2. The formation constant K_f for POFs in n-hexane, chloroform and methanol drastically decreased with the increase in polarity, thus illustrating the important role of solvents in iodine binding.

Introduction

Nuclear power is an important and widely used energy source due to its ultrahigh energy density and low carbon emissions. However, nuclear waste containing radioactive material is an inevitable product of nuclear power generation. Appropriate management of such waste is the key to the application of clean, safe, and responsible nuclear energy.[1] The radionuclides ^{129}I and ^{131}I are two of the main components of waste streams. They are generated within fuel rods through the fission of uranium atoms during the operation of nuclear reactors, and they can disperse rapidly in air and contaminate liquid and solid waste-processing systems. The half-lives of ^{131}I and ^{129}I are about 8 days and 15.7 million years, respectively, both can be ingested in food or water, affecting human metabolic processes. The 2011 disaster at Japan's Fukushima Dai-Ichi nuclear energy centre is proof that we are still far from being able to safely control nuclear energy. The elevated concentrations of radioactive cesium and iodine subsequently found in small fish several dozen miles south of Fukushima, and the high levels of radioactivity in the seawater 25 miles offshore, are a reminder that the effective capture and storage of nuclear waste in air and in liquid and solid systems are equally important to public safety. Hence, several projects aimed at capturing iodine have been undertaken, including wet scrubbing and the use of porous materials.[2] However, each of these methods has several technical challenges that need to be overcome. Stable, effective, high-iodine storage capacity materials have yet to be discovered. In addition, understanding the adsorption behaviour in air, liquid, and solid states remains a challenge. We believe that these issues can be addressed by using porous organic frameworks (POFs)[3] that feature high surface areas and physicochemical stability as storage media. Given the growing interest in exploring the molecular basis for iodine capture in POFs, an investigation of the factors that influence the iodine loading amount and efficiency, especially the interactions or synergism between the guests and the host framework, is required.

A *dia* topology robust all-carbon scaffold PAF-1[3f] with ultrahigh surface area (S_{BET} = 5600 m^2 g^{-1}) and physicochemical stability (up to 420 °C) is an ideal material with which to conduct an iodine adsorption study. The high surface area and accessible pore volume (total pore volume = 2.63 cm^3 g^{-1}, micropore volume = 0.89 cm^3 g^{-1}) supply an adequate void for iodine or iodide, and the uniform micropores (1.48 nm) shuttle the small molecular guests and improve the diffusion rates. In addition, its impressive physicochemical stability expands its potential applicability to a wide variety of areas. Another POF with *hcb* topology, JUC-Z2[4] (composed of triphenylamine moieties), also exhibits high thermal stability (430 °C), high surface area (S_{BET} = 2081 m^2 g^{-1}), uniform micropores (1.18 nm), and open pore volume (total pore volume = 1.45 cm^3 g^{-1}, micropore volume = 0.40 cm^3 g^{-1}). The effective low molecular weight binding sites of the N atom lead to relatively high interactions with guest molecules.[4b] Furthermore, the intense electron density of N makes JUC-Z2 a Lewis base, which results in forced interaction with Lewis acid iodine and the possible exchange of electrons to a stable state. These two typical POFs were used as model compounds to explore the mechanism of iodine sorption in pure organic open frameworks.

In the current study, the iodine was introduced by diffusion in low concentration iodine vapor followed by guest binding in an iodine solution with a different polarity. Two different strategies for host-guest interaction studies were used in these systems. To calculate the isosteric enthalpy at zero surface coverage using a virial equation,[5] two iodine vapor sorption isotherms at different temperatures are required. However, the

special nature of iodine, specifically its violent reaction with some metals and relatively low vapor pressure against gases in measurement conditions, make it impossible to collect iodine vapor sorption isotherms with the traditional commercial gas/liquid sorption instruments. Thus, the micro-spring balance of a McBain-Bakr-type[6] quartz fiber (Figure 1) was used to measure the uptake gravimetrically at different temperatures while studying the adsorption behavior of the iodine vapor. As a result, surface area and pore volume play an important role in iodine vapor sorption. Guest binding studies were also carried out in iodine solutions with different polarities. The effect of iodine concentrations in solvents was measured. The formation of a constant K_f in the complexes, and the number of guests per unit of formula for a host solid, were obtained and thus a trend in host-guest interaction strength was also revealed.
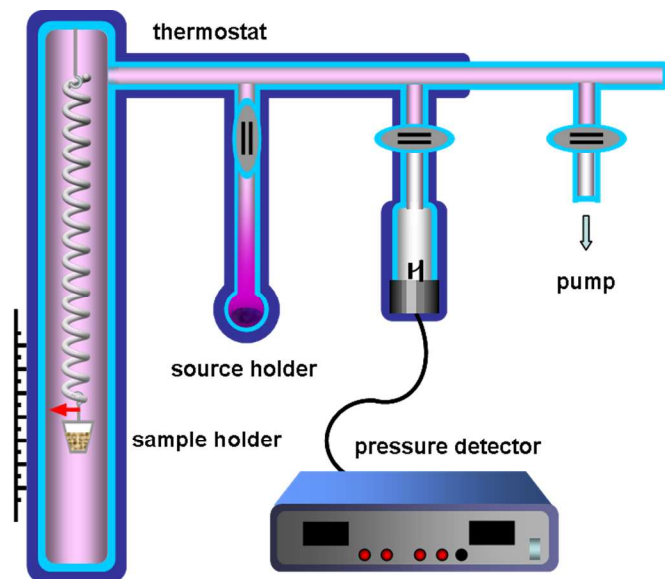
Figure 1. Apparatus used in iodine vapor storage measurements.

Experimental

Materials and Synthetic Procedures

The starting materials and dehydrated solvents were purchased from Aldrich Chemicals.
Tetrakis(4-bromophenyl)methane $(BrC_6H_4)_4C$ was prepared according to the previous literature.[7] PAF-1 and JUC-Z2 were prepared according to the previous literature.[3f, 4a]

Instruments

UV-Vis, FTIR and Raman Spectroscopy Experiments. UV-Vis spectra were recorded using a quartz cell of 1 cm path length on a SHIMADAZU UV-2450 spectrophotometer with the same solvent in the examined solution as a blank. The FTIR spectra (KBr) were measured using a SHIMADZU IRAffinity-1 Fourier transform infrared spectrometer. Raman spectra were acquired using an H. J. Y LabRAM Aramis equipped with a 532 nm diode laser.
Gas Chromatographic Experiments. Gas chromatographic (GC) experiments were conducted using a SHIMADAZU GC-2014C, which was fitted with a 30 m × 0.25 mm × 0.25 μm cross-linked poly(ethylene glycol) capillary column and interfaced with a GC Light Real Time Analysis. A flame ionization detector was used.

Iodine Vapor Sorption Measurements. The vacuum swing adsorption process was undertaken in an iodine vapor storage apparatus, and iodine uptakes were measured gravimetrically. Samples of a known weight (about 100 mg) were loaded into a sample holder and the apparatus was then sealed to prevent exposure to air and atmospheric moisture during the measurement. The source holder was filled with ultra-high-purity grade iodine (99.999 %) and the cock was closed. A low iodine vapor pressure was maintained by cooling the holder in a liquid nitrogen bath. After evacuation (P < 0.05 Pa), a little iodine vapor was diffused into the system. The system pressure and the elongation of the spring were observed and recorded until a state of equilibrium was reached. This operation was repeated to obtain the spring length under different system pressures. The iodine sorption isotherms at 273 K were measured in an ice-water bath.

To calculate the coverage-dependent isosteric heat of sorption, the data were modeled with a virial-type expression composed of empirical parameters a_i and b_j, which were independent of temperature:[5]

$$\ln(p) = \ln(n) + (1/T)\sum_{i=0}^{m} a_i n^i + \sum_{j=0}^{n} b_j n^j \tag{1}$$

where p is pressure, n is the amount adsorbed (or uptake), T is the temperature, and a_i and b_j determine the number of terms required to adequately describe the isotherm. Successive terms were included in the fitting expression until they did not appreciably reduce the goodness-of-fit. In all cases, $a_i \leqslant 6$ and $b_j \leqslant 3$. Based on these results, the isosteric heat of adsorption was calculated according to the following equation:

$$Q_{st} = -R\sum_{i=0}^{m} a_i n^i \tag{2}$$

where R is the gas constant.
Fixed pressure iodine sorption measurements. The activated samples (100 mg) were placed in a sealed vessel with excess solid iodine, which was used to support fixed iodine vapor pressure. The loading of the porous materials measured gravimetrically after different exposure times at 333 K. Competitive iodine/water vapor sorption experiments were conducted at the same condition. Activated sample was sealed with excess iodine and water in an adsorption chamber and placed in the oven at 333 K. The saturated vapor pressure of iodine and water at this temperature is 571 Pa and 26163 Pa respectively.
Binding of PAF-1, JUC-Z2 with iodine/organic solvent solution. As-synthesized PAF-1 and JUC-Z2 samples were first degassed at 423 K under vacuum for 10 h. The accurately measured solid samples (about 30 mg) were immersed in the measured volume of anhydrous organic solvent solutions containing iodine for 10 h at 302 K. The initial guest concentrations $([G]_0)$ of iodine varied as follows: PAF-1 and JUC-Z2 varied from 1.382×10^{-4} to 1.430×10^{-3} M to maintain the saturation (θ) values within the 15-73% range in the iodine/n-hexane system; 1.508×10^{-4} to 1.474×10^{-3} M to maintain the saturation (θ) values within the 15-66% range in the iodine/chloroform system; and 1.428×10^{-4} to 1.596×10^{-3} M to maintain the saturation (θ) values within the 4-53% range in the iodine/methanol system. The guest concentration change was measured by UV-Vis spectrum, and the data were fitted to Equation (4). The formation constant (K_f) for the host-guest complexes formed between a binding site (BS) on the insoluble hosts and a guest molecule (G) were defined as k_{ad}/k_{de} [Eq. (3)] by analogy with the Langmuir isotherm for adsorption of gas

molecules on solid surfaces. The concentration of G bound to BS ([BS•G]) against [G] was plotted. The K_f and $[BS]_0$ values were estimated by analyzing the data according to Equation (4).

$$BS + G \frac{k_{ad}}{k_{de}} BS \cdot G$$

$$K_f = \frac{k_{ad}}{k_{de}} = \frac{[BS \cdot G]}{[BS][G]} \quad (3)$$

If θ is defined as fractional coverage,

$$\theta = \frac{[BS \cdot G]}{[BS]_0} = \frac{[G]}{([G] + 1/K_f)}$$

Then

$$[BS \cdot G]/\omega = \frac{([BS]_0/\omega)[G]}{([G] + 1/K_f)} \quad (4)$$

where ω is the amount of host solid per unit volume of the solution (mg mL^{-1})

$$\Delta_r G_m = -RT \ln K \quad (5)$$

Binding of PAF-1, JUC-Z2 with methanol/n-hexane and chloroform/n-hexane solutions. As-synthesized samples were degassed at 423 K under vacuum for 10 h. The accurately measured solid samples (about 30 mg) were immersed in the measured volume of anhydrous n-hexane solution containing methanol and chloroform, respectively, for 10 h at 302 K. The initial guest concentration ($[G]_0$) of methanol varied from 0.05 to 0.21 M for PAF-1 and JUC-Z2, and that of chloroform from 0.2 to 1.5 M to maintain the saturation (θ) values within the 20-80% range. The guest concentration change was measured by GC spectrum, and the data were fitted to Equation (4).

Results and discussion

Iodine Vapor Sorption in POFs

Gravimetric measurements were performed on the iodine vapor adsorption equilibrium state while the pressure was raised from about 5×10^{-2} Pa to the saturation vapor pressure[8] (vacuum swing adsorption). Upon exposure to the iodine vapor, the activated sample became gradually darker and diffused from the surface to the bottom. In addition, the loading equilibrium state was reached in 15 minutes due to the gravimetric detection, with the system attaining the saturation vapor pressure in around 10 h. The iodine release and recovery process was carried out in vacuum and heating conditions. Given the diffusion rate and physical stress, which may be followed by a redox reaction between the host and guest, the desorption process required more time and the fading began at the surface. Figure 2A shows that the iodine uptake of PAF-1 increased almost linearly with the increase in vapor pressure, both at 298 K and 310 K. The reduced sorption at relatively higher temperatures meant that the fitting provided estimates of the Q_{st} at low coverage only. As Figure 2C shows, the isosteric heat of adsorption of the 3D all-carbon framework PAF-1 increased smoothly from -14.9 kJ mol^{-1} to -33.3 kJ mol^{-1}. The rising trend indicates that adsorbate-adsorbate interactions cannot be neglected in low coverage. This trend coincided with the almost linear pattern of iodine vapor sorption in PAF-1, which indicates that the binding energy between an iodine guest

and the framework's host is as low as Van der Waals' force, and the adsorption energy of the first layer of iodine is similar to the interaction between adsorbates. Although the iodine heat of adsorption is not high, having an ultrahigh surface area still gave PAF-1 a significant sorption capacity of 1.86 g g^{-1}, which corresponds to 65 wt% at extremely low pressure as 40 Pa and 298 K. Comparatively, the iodine vapor uptakes outperformed those of all previously reported porous materials (Table 1). Hence, PAF-1 shows the highest iodine vapor uptakes to date in such low pressure measurement conditions (40 Pa, corresponding to 3.95×10^{-4} atm).
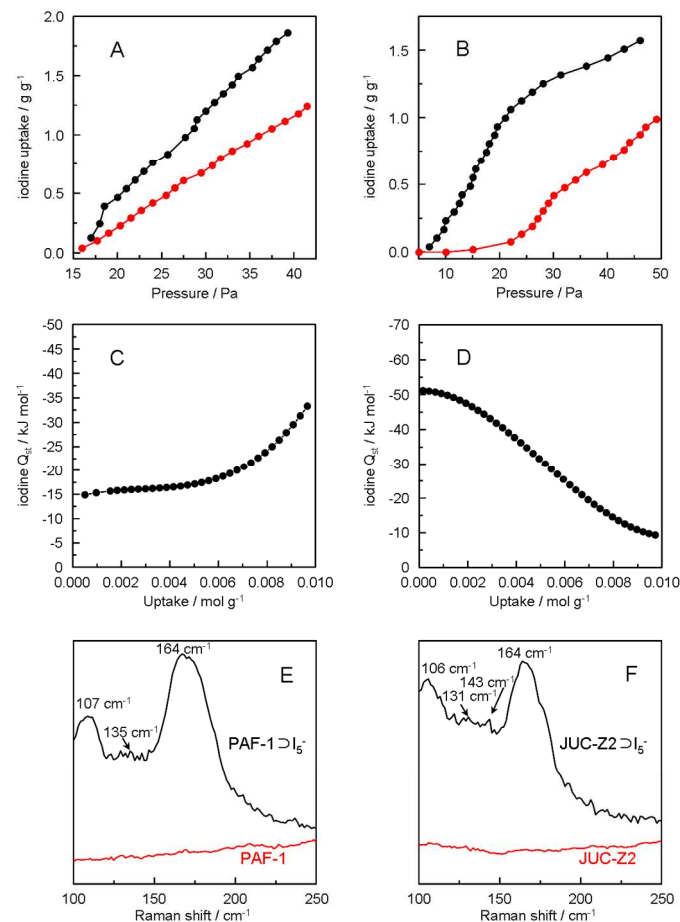
Figure 2. (A) iodine vapor adsorption isotherms of PAF-1 at 298 K (black) and 310 K (red); (B) iodine vapor adsorption isotherms of JUC-Z2 at 298 K (black) and 313 K (red); (C) Q_{st} for iodine vapor of PAF-1 calculated with the sorption isotherms at 298 K and 310 K; (D) Q_{st} for iodine vapor of JUC-Z2 calculated with the sorption isotherms at 298 K and 313 K. (E) Raman spectrum of iodine-loaded PAF-1 obtained by vacuum swing adsorption process (PAF-1 $\supset$ I$_5^-$, black) and PAF-1 (red); (F) Raman spectrum of iodine-loaded JUC-Z2 obtained by vacuum swing adsorption (JUC-Z2 $\supset$ I$_5^-$, black) and JUC-Z2 (red) over a wavelength reduced range.

Unlike iodine adsorption in PAF-1, the iodine uptake in JUC-Z2 at 298 K and 313 K exhibited type V adsorption curves, which meant that the adsorption energy of the first layer of iodine was smaller than the interaction between adsorbates (Figure 2B). In contrast, the heat of sorption at low coverage for JUC-Z2 was -51.1 kJ mol^{-1}, which was over three times higher than that of PAF-1, indicating that the N atom is a very

Table 1. Summary of BET surface areas and iodine sorption properties of porous materials series

| | | | iodine sorption | | |
sample	S_{BET} (m^2 g^{-1})	method	T (K)	iodine uptake (wt%[a])	reference
zeolite 5A	-	vacuum swing adsorption	309[b]	5.65 molecules per unit cell	6b
PAF-1	5600	vacuum swing adsorption	298	65.0[c]	this work
PAF-1	5600	fixed vapor pressure	333	74.2	this work
JUC-Z2	2081	vacuum swing adsorption	298	59.0[c]	this work
JUC-Z2	2081	fixed vapor pressure	333	80.4	this work
ZIF-8	1630	fixed vapor pressure	350	55.6	2b
HKUST-1	1500-2100	fixed vapor pressure	348	63.6	9
$\{[(CuI)_2(2)]\}_n$	-	fixed vapor pressure	r. t.[d]	52.4	10
$\{[Cu_6(pybz)_8(OH)_2]\bullet I_5^-\bullet I_7^-\}_n$	-	hydrothermal synthesis	413	43.2	11
$[Zn_7(L1)_3(H_2O)_7]_n\cdot[Zn_5(L1)_3(H_2O)_5]_n\cdot xSolvent$	373	iodine sorption in solution	r. t.	$1\cdot2.65I_2$	12
$[Zn(C_6H_8O_8)]\approx2H_2O$	-	fixed vapor pressure	292	14.3	13
$[Cu(IN)_2]$ (IN: isonicotinato)	-	hydrothermal synthesis	413	45.2	14
M(TCNQ) (M = Na, K)	-	fixed vapor pressure	r. t.	$M(TCNQ)\cdot I_6$	15
CC3	624	fixed vapor pressure	293	35.8	16
$[Zn_3(DL\text{-}lac)_2(pybz)_2]\bullet3I_2$	763	iodine sorption in solution	r. t.	49.7	17
Polyurethane (PU1)	-	fixed vapor pressure	343	56.5	18
TPP	-	iodine sorption in solution	353-373	26.4-29.3	19
L-leucyl–L-serine	-	iodine sorption in solution	r. t.	3.8	20
$[Fe_3(HCOO)_6](I_2)_{0.84}$	385	fixed vapor pressure	r. t.	32.8	21
$[WS_4Cu_4(4,4'\text{-}bpy)_4]\cdot[WS_4Cu_4I_4(4,4'\text{-}bpy)_2]$	-	iodine sorption in solution	r. t.	32.9	22

[a] wt% = iodine mass / (sample mass + iodine mass); [b] Zeolite 5A adsorbed iodine at 85 °C in the first day. The temperature was reduced gradually to 36 °C in four more days and increased to 50 °C on the sixth day, by which time 5.65 molecules per unit cell were adsorbed; [c] Iodine uptake was recorded at 40 Pa; [d] Room temperature abbreviate as r. t..

effective binding site for iodine (Figure 2D). The rise in coverage prompted the isosteric heat to drop off considerably to about -9.4 kJ mol^{-1}. Although the isosteric heat of JUC-Z2 was higher than that of PAF-1 at very low coverage due to the effective N binding sites, but it decreased when coverage increased, and far less than that of PAF-1 at higher coverage. This indicates that strong binding sites exist in the electron-rich JUC-Z2, causing forceful interactions between the guest and host at the beginning of iodine adsorption.[5b] It is possible that the constricted structure of JUC-Z2 overlaps the energy potentials, which promotes the adsorbent-adsorbate interaction at very low iodine coverage. Overall, small pore dimensions, the electronic character of the N-containing framework, surface areas, and void pore volume all influence iodine vapor sorption. In low coverage, an effective binding site is very important, and it leads to the high interaction between iodine molecules, while the total uptakes are mainly influenced by the surface area at higher coverage. Therefore, the total iodine uptake of JUC-Z2 at 298 K is lower than that of PAF-1.

coverage. Normally, there are two possible assembly strategies for forming I_5^- combined with I_2, I^-, I_3^- units and I…I bond interactions during an adsorption procedure. The characteristic peaks at around 106 cm^{-1}, 135 cm^{-1} and 164 cm^{-1} belong to both perturbed di-iodine molecules and asymmetric I_3^- ions for polyiodides $[I_3^-\bullet I_2]$, whereas the peaks at about 143 cm^{-1} and 164 cm^{-1} are the result of perturbed di-iodine units for $[I^-\bullet(I_2)_2]$.[24] Hence, in the desorption process, two decomposition reactions of polyiodide anions can occur: $I_5^- \rightarrow 2I_2 + I^-$ or $I_5^- \rightarrow I_2 + I_3^-$.[25] This coincides with the iodine vapor desorption behavior, which is slow but complete. In contrast, it has been reported that the nature (shape, size, and charge) of the network plays a crucial role in the structural and geometrical features of the polyiodide.[26] Our results indicate that although PAF-1 exhibits *dia* topology while JUC-Z2 shows *hcb* topology, but both of them template the fabrication of I_5^-.(Figure 3)

Figure 3. Method for introducing iodine by diffusion in iodine vapor.
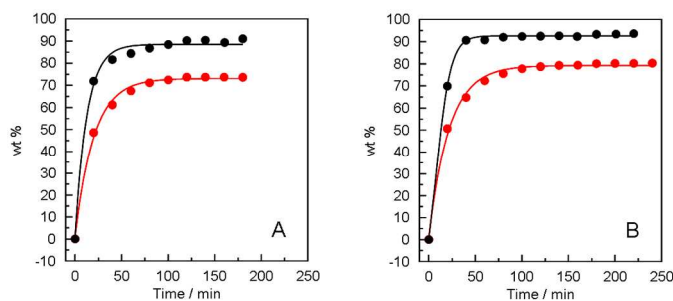
Figure 4. Gravimetric iodine uptake in dry condition (red) and humility condition (black) of (A) PAF-1 and (B) JUC-Z2 as a function of time at 333 K.

The structure of the iodine inside the pores of the POFs was revealed by Raman spectroscopy (Figure 2E and 2F). The strong peak located at 165 cm^{-1}, exhibited in the Raman spectra of both PAF-1 and JUC-Z2, consisted of I_5^-.[11, 17, 23] This may indicate that the charge transfer occurred between the guest iodine molecules and the electron-rich host network at high

To further explore iodine vapor sorption, gravimetric measurements were taken in another strategy with a fixed iodine pressure. The color of the sample changed gradually from off-white to dark brown with increasing time. Figure 4 shows the weight of the samples at various time intervals. The mass of the sample increased significantly within the first 100

minutes, whereas the rate at which the mass rose slowed down as the pores became occupied by guest molecules and the saturation of surface adsorption. After 200 minutes, the iodine uptake values (iodine weight/(sample weight + iodine weight)) for PAF-1 and JUC-Z2 were 74.2 wt% and 80.4 wt%, respectively – significantly higher than those mentioned at 40 Pa / 298 K. Hence, iodine accumulation occurred not only in the pores, but also at the outer surface once the pores were filled. This high surface adsorption phenomenon has been observed in the iodine sorption process of ZIF-8[2b] and porous organic cages,[16] which may also be useful in real iodine sorption applications. The iodine sorption capacity obtained by thermal analysis is 64 wt% and 73 wt% for PAF-1 and JUC-Z2. Taking into account the loss of iodine in the sample transfer, the result coincides with the data get from the gravimetric sorption. (Figure S1 and Figure S2) Comparatively, we took the iodine vapor sorption measurement on activated carbon in the same condition, the uptake values 49.3 wt%.(Figure S3) It demonstrated that this frequently used commercial adsorbent lose advantage in iodine vapor sorption application. Considering the actual industry application of iodine sorption process, we further detected the iodine sorption capacity in humility condition. As shown in Figure 4 (black), the total weight increase contains both the iodine uptake and water uptake. Based on the iodine mass obtained in dry condition, the quantity of water loaded was calculated by the subtraction. The derived iodine/water selectivity of PAF-1 is 5.1 after 200 minutes exposure. However, the water sorption value of JUC-Z2 is lower than that of PAF-1, which leads to a higher iodine/water selectivity (6.5). In conclusion, PAF-1 and JUC-Z2 could sorption iodine over water. Furthermore, the physicochemical stability of them leads to the application of capture iodine in presence of water reversible.

Iodine Adsorption in PAF-1 and JUC-Z2 in Solution
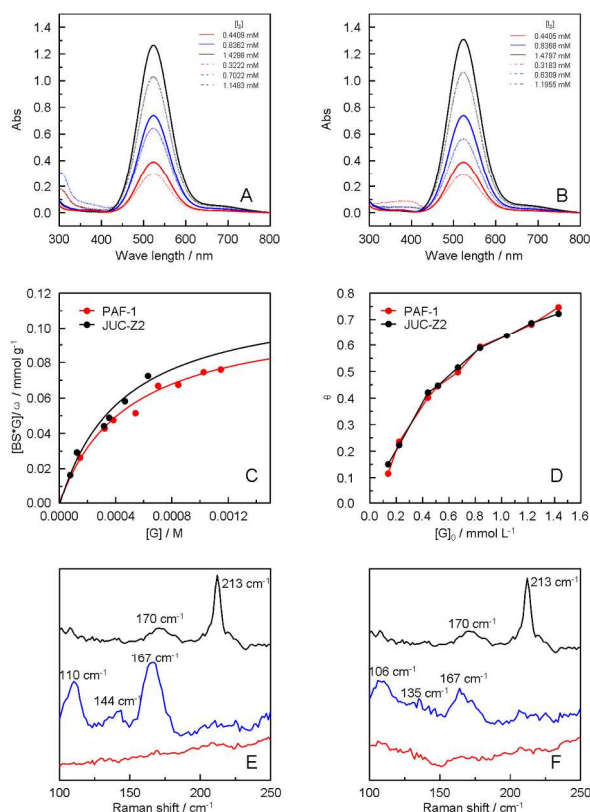
Figure 5. (A) UV-Vis spectra recorded in iodine absorbance mode in n-hexane (actual line) and iodine/n-hexane with PAF-1 stirring for 10 h at R.T. (dotted line); (B) UV-Vis spectra recorded in iodine absorbance mode in n-hexane (actual line) and iodine/n-hexane with JUC-Z2 stirring for 10 h at R.T. (dotted line); (C) Binding of host solid PAF-1 (red) and JUC-Z2 (black) with iodine; (D) Changes in fractional coverage θ when the equilibrium for the host ± guest complex formation was attained, according to the different original concentrated iodine/n-hexane solution; (E) Raman spectra of iodine/n-hexane solution (black), iodine-loaded PAF-1 obtained by iodine sorption in n-hexane solution (blue) and PAF-1 (red);　(F) Raman spectra of iodine/n-hexane solution (black), iodine-loaded JUC-Z2 obtained by iodine sorption in n-hexane solution (blue) and JUC-Z2 (red).

To explore the iodine uptakes and adsorption in PAF-1 and JUC-Z2 in the solution state, we also studied the host-guest interaction between POFs and iodine in organic solution. In these systems, polar solvents act as Lewis bases, and charge-transfer complexes form when iodine is dissolved in them. The energy distribution of iodine's molecular orbital is changed. Hence the solutions are brown. When iodine is dissolved in non-polar solvents such as n-hexane, the iodine is violet in color.[27] To comprehensively study the binding properties of PAF-1 and JUC-Z2 in iodine solution, we chose n-hexane, chloroform, and methanol as solvents because their polarities cover a range from 0.06 (n-hexane) to 6.6 (methanol). First, we studied the influence of binding time on changes in concentration. The UV-Vis absorbance peaks detected and calculated for iodine in n-hexane were 523 nm (Figures 5A and 5B). The binding process was carried out on the activated samples at room temperature. As the duration of the binding process increased, the absorbance at 523 nm noticeably decreased. However, this prolonged duration called attention to some indefinite factors in the measurements, such as the volatilization of the organic solvent and the iodine. The rate at which the absorbance decreased slowed as the pores became occupied with the guest after 10 h (Figure S5). Finally, we defined the conditions of the iodine solution experiments by dispersing 30 mg activated samples in the anhydrous solutions of iodine with various initial concentrations of the guest ($[G]_0$) until equilibrium was reached (about 10 h). The absorbance changes for the iodine solution were then monitored by UV spectrophotometry.

The absorbance of iodine in n-hexane increased linearly with the rise in concentration, and was empirically adjusted as a zero-order equation (Figure S4). The interactions between iodine and PAF-1 and JUC-Z2 were plotted using [BS•G] (the concentration of G bound to BS) against [G] and are illustrated in Figure 5C. The data were then fitted to Equation (4) to obtain the formation constant (K_f) and the maximum amount (mole) of iodine ($[BS]_0/\omega$) (Table 2). An analysis of the data provided K_f = 2080.2 M^{-1} and $[BS]_0/\omega$ = 0.11 mmol g^{-1} for PAF-1, and K_f= 2276.8 M^{-1} and $[BS]_0/\omega$ = 0.12 mmol g^{-1} for JUC-Z2 at 302 K. These values of $[BS]_0/\omega$ indicated that the host solids, PAF-1 and JUC-Z2, had 0.28 and 0.23 binding sites, respectively, for the iodine molecule per formula of the solid. It is evident that JUC-Z2's binding affinity for iodine is similar to that of PAF-1, and they have a similar capacity for iodine in n-hexane solution. Figure 5D illustrates the correlation between the saturation (θ) values and initial concentrations of iodine/n-hexane solution, demonstrating that the high fractional coverage   values   obtained

Table 2. Inclusion of host solids PAF-1 and JUC-Z2 with iodine in various solvent systems

Solvent	PAF-1			JUC-Z2		
	K_f / M^{-1}	$\Delta_rG_m(T)^a$ / kJ mol^{-1}	$[BS]_0/\omega$ / mmol g^{-1}	K_f / M^{-1}	$\Delta_rG_m(T)^a$ / kJ mol^{-1}	$[BS]_0/\omega$ / mmol g^{-1}
N-hexane	2080.2	-19.2	0.11	2276.8	-19.5	0.12
Chloroform	1339.0	-18.1	0.05	1347.1	-18.1	0.07
Methanol	733.2	-16.4	0.04	746.3	-16.4	0.03

a $\Delta_rG_m(T)$ is calculated with equation 5

at the high initial concentration were similar in the binding processes of PAF-1 and JUC-Z2.
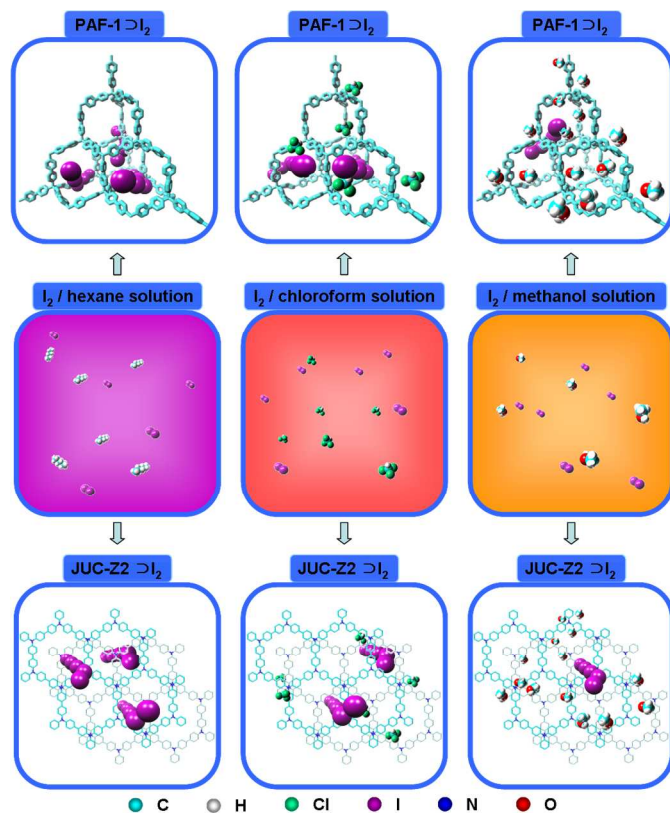
Figure 6. Method for introducing iodine by iodine sorption in organic solution.

For detect the structure of iodine which adsorbed in PAF-1 and JUC-Z2, Raman spectroscopy were taken on these materials prepared via iodine sorption in solution process. The peak at 213 cm^{-1} in iodine/n-hexane solution (black line) attributed to $\upsilon 1$ symmetric mode for gaseous iodine, while no obvious peak can be seen about PAF-1 and JUC-Z2 (red line). However, after the iodine sorption in n-hexane solution, iodine loaded PAF-1 and iodine loaded JUC-Z2 exhibit three peaks characterized I_5^-. (blue line in Figure 5E and Figure 5F) As shown in Figure 5E, the peaks at 110 and 167 cm^{-1} correspond to the $\upsilon 1$ of a triiodide and weakly coordinated iodine, respectively. The peak at 144 cm^{-1} attributed to an asymmetric triiodide.[11, 17, 23] Hence the I_5^- formed in PAF-1's framework is mainly shown as V shape ($[I^- \bullet (I_2)_2]$). However, the result of JUC-Z2 in Figure 5F is different from PAF-1. Peaks at 106 cm^{-1}, 135 cm^{-1} and 167 cm^{-1} show that L shape I_5^- ($[I_3^- \bullet I_2]$) formed in the iodine loaded JUC-Z2.[11, 17, 23] (Figure 6) I_5^- might be charge-transferred and formatted during the sorption process.
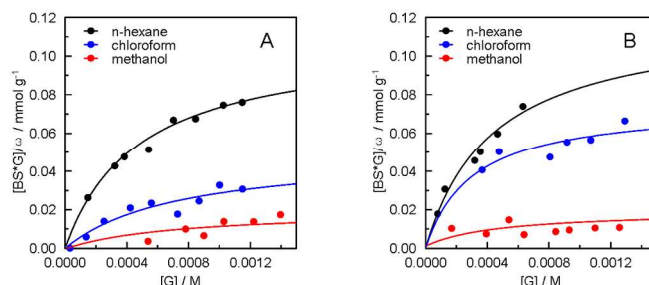
Figure 7. (A) Binding of host solid PAF-1 with iodine in n-hexane (black), chloroform (blue) and methanol (red); and (B) Binding of host solid JUC-Z2 with iodine in n-hexane (black), chloroform (blue) and methanol (red).
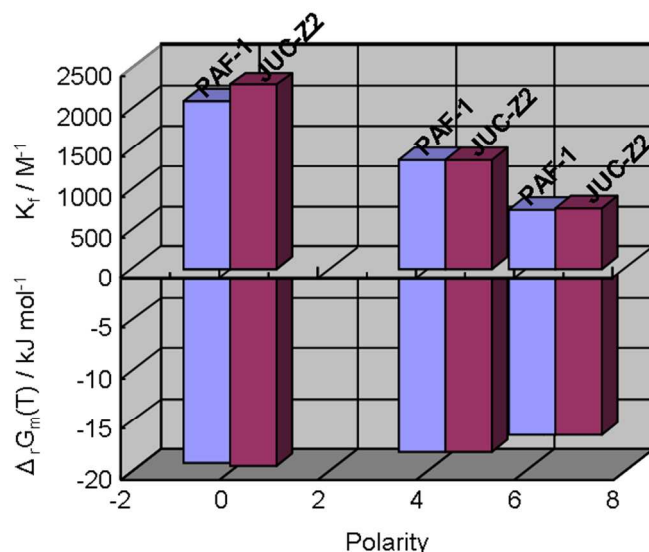
Figure 8. The relationships among the polarities of the organic solvents, the binding constants (K_f) and Gibbs free energy ($\Delta_rG_m(T)$).

Using the same experimental procedure, we studied the binding of PAF-1 and JUC-Z2 with iodine/chloroform and iodine/methanol solutions. When the host materials were immersed in iodine organic solvent for 10 h at room temperature, the iodine concentration measured by UV-Vis spectrophotometry decreased sharply in the n-hexane system, moderately in chloroform, and slightly in methanol.(Figure S10-S19) Separation peaks software was used to resolve the problem of overlapping iodine and solvent signals. The Langmuir isotherm curves are shown in Figure 7, and K_f, $[BS]_0/\omega$ were estimated by fitting the corresponding data to Equation (4). The binding constants (K_f) of PAF-1 were in the following order: iodine in n-hexane (2080.2 M^{-1}) > in chloroform (1339.0 M^{-1}) > in methanol (733.2 M^{-1}) (Table 2). The K_f value of PAF-1 in n-hexane was nearly twice as high as

Journal Name

ARTICLE

Table 3. Inclusion of host solids PAF-1 and JUC-Z2 with methanol and chloroform in n-hexane

Host	Guest	K_f/ M^{-1}	$\Delta_r G_m(T)^a$ / kJ mol^{-1}	$[BS]_0/\omega$ / mmol g^{-1}
PAF-1	Chloroform	1.86	-1.6	6.23
	Methanol	7.80	-5.1	13.93
JUC-Z2	Chloroform	3.17	-2.9	6.89
	Methanol	9.10	-5.5	19.05

[a] $\Delta_r G_m(T)$ is calculated with equation 5

that in chloroform, and four times higher than that in methanol. It should be noted that the trend of binding affinity coincided with the polarities of these organic solvents (Figure 8). In addition, the K_f value of JUC-Z2 exhibited the same results (the K_f values in n-hexane, chloroform and methanol were 2276.8 M^{-1}, 1347.1 M^{-1} and 746.3 M^{-1}, respectively). This is probably due to the retarded binding prompted by the stronger interaction between the polar solvents and the iodine. Moreover, in terms of the K_f value, JUC-Z2 exhibited a binding tendency that was similar to that of PAF-1, despite their differences in chemical structure, framework topologies, surface area, and pore size distribution. An analysis of the data also provided the maximum amount (mole) of iodine ($[BS]_0/\omega$) adsorbed in the pores: 0.11, 0.06, and 0.04 mmol g^{-1} for PAF-1 in n-hexane, chloroform, and methanol, respectively; and 0.12, 0.07, and 0.03 mmol g^{-1} for JUC-Z2, respectively.
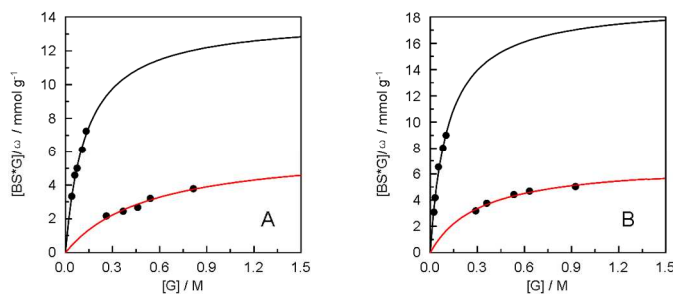
Figure 9. (A) Binding of host solid PAF-1 with methanol (black) and chloroform (red) in n-hexane; (B) Binding of host solid JUC-Z2 with methanol (black) and chloroform (red) in n-hexane.

The competition between iodine and organic solvent was carried out on the binding sites of the host porous materials, and parts of those binding sites may be occupied by solvent molecules in polar systems. Hence the binding capacity decreased with the increase of a solvent's polarity in PAF-1 and JUC-Z2. To prove this, we explored the adsorption of solvents such as chloroform and methanol in POFs. PAF-1 and JUC-Z2 were immersed in n-hexane that contained a measured amount of methanol and chloroform. As the binding of the POF with the non-polarity of the n-hexane was very weak, we assumed that there was no interaction between n-hexane and the POFs. The concentrations of the methanol and chloroform were monitored by GC measurements when the porous materials were immersed in the mixture solution for 24 h. The plots of [BS•G] against [G] for PAF-1 and JUC-Z2 in the methanol/n-

hexane and chloroform/n-hexane solutions, respectively, are illustrated in Figure 9. K_f and $[BS]_0/\omega$ were estimated by fitting the corresponding data to Equation (4) (summarized in Table 3). The result indicated that apart from the size-fit with the host cavity and the adequate space for guest molecules, the adsorption of chloroform and methanol in the POFs was similar. However, the binding constant, and therefore the amount of methanol binding in the host cavity, was more than that of chloroform in the POFs. This is consistent with the conclusion that less iodine was adsorbed by the host pores in the iodine/methanol system than in the iodine/chloroform system. The K_f values demonstrated that both PAF-1 and JUC-Z2 exhibited enhanced binding trends with higher polarity organic solvents in the following order: methanol > chloroform > n-hexane.

Conclusions

In conclusion, we investigated the iodine sorption of PAF-1 and JUC-Z2 in both an iodine vapor system and in iodine solutions with different polarities. The results suggest that a large surface area and pore volume facilitate the uptake capacity of iodine vapor in low pressure conditions. In addition, the small pore size and electronic character of the N-containing framework of JUC-Z2 assisted the interaction between host and guest compounds at very low coverage in vapor adsorption. As a result, PAF-1 exhibits the highest iodine vapor uptakes among all previously reported porous materials. Furthermore, PAF-1 and JUC-Z2 can sorption iodine vapor over water vapor. In contrast, the iodine adsorption in solution exhibited different behavior compared to that observed in vapor. The binding constants (K_f), while greatly affected by the polarity of the solvent, were not influenced by the pore structure or surface area of the POFs. These results on the structure-property relationships have the potential to act as the basis for future experimental syntheses, and could lead to new functional porous material designs for iodine loading.

Acknowledgements

Notes and references

a State Key Laboratory of Inorganic Synthesis and Preparative Chemistry, Jilin University, Changchun, China.

b Department of Chemistry, Jilin University, Changchun, China.

* sqiu@jlu.edu.cn; tben@jlu.edu.cn

1   N. R. Soelberg, T. G. Garn, M. R. Greenhalgh, J. D. Law, R. Jubin, D. M. Strachan, and P. K. Thallapally, *Sci. Technol. Nucl. Ins.*, 2013, **2013**, 702496.

2   a) K. W. Chapman, P. J. Chupas, and T. M. Nenoff, *J. Am. Chem. Soc.,* 2010, **132**, 8897; b) D. F. Sava, M. A. Rodriguez, K. W. Chapman, P. J. Chupas, J. A. Greathouse, P. S. Crozier, and T. M. Nenoff, *J. Am. Chem. Soc.,* 2011, **133**, 12398; c) K. W. Chapman, D. F. Sava, G. J. Halder, P. J. Chupas, and T. M. Nenoff, *J. Am. Chem. Soc.,* 2011, **133**, 18583; d) D. F. Sava, T. J. Garino, and T. M. Nenoff, *Ind. Eng. Chem. Res.*, 2012, **51**, 614.

3   a) J. Jiang, F. Su, A. Trewin, C. D. Wood, N. L. Campbell, H. Niu, C. Dickinson, A. Y. Ganin, M. J. Rosseinsky, Y. Z. Khimyak, and A. I. Cooper, *Angew. Chem. Int. Ed.,* 2007, **46**, 8574; b) S. Wan, J. Guo, J. Kim, H. Ihee, and D. Jiang, *Angew. Chem. Int. Ed.,* 2008, **47**, 8826; c) P. Kuhn, M. Antonietti, and A. Thomas, *Angew. Chem. Int. Ed.,* 2008, **47**, 3450; d) N. B. McKeown, P. M. Budd, K. J. Msayib, B. S. Ghanem, H. J. Kingston, C. E. Tattershall, S. Makhseed, K. J. Reynolds, and D. Fritsch, *Chem. Eur. J.*, 2005, **11**, 2610; e) A. P. Côté, A. I. Benin, N. W. Ockwig, M. O'Keeffe, A. J. Matzger, and O. M. Yaghi, *Science,* 2005, **310**, 1166; f) T. Ben, H. Ren, S. Ma, D. Cao, J. Lan, X. Jing, W. Wang, J. Xu, F. Deng, J. M. Simmons, S. Qiu, and G. Zhu, *Angew. Chem. Int. Ed.,* 2009, **48**, 9457.

4   a) T. Ben, K. Shi, Y. Cui, C. Pei, Y. Zuo, H. Guo, D. Zhang, J. Xu, F. Deng, Z. Tian, and S. Qiu, *J. Mater. Chem.,* 2011, **21**, 18208; b) C. Pei, T. Ben, Y. Cui, and S. Qiu, *Adsorption,* 2012, **18**, 375.

5   a) L. Czepirski, and J. Jagiello, *Chem. Eng. Sci.,* 1989, **44**, 797; b) J. L. C. Rowsell, and O. M. Yaghi, *J. Am. Chem. Soc.,* 2006, **128**, 1304; c) A. Anson, J. Jagiello, J. B. Parra, M. L. Sanjuan, A. M. Benito, W. K. Maser, and M. T. Martinez, *J. Phys. Chem. B,* 2004, **108**, 15820; d) B. Chen, X. Zhao, A. Putkham, K. Hong, E. B. Lobkovsky, E. J. Hurtado, A. J. Fletcher, and K. M. Thomas, *J. Am. Chem. Soc.*, 2008, **130**, 6411.

6   a) J. W. McBain, and A. M. Bakr, *J. Am. Chem. Soc.,* 1926, **48**, 690; b) K. Seff, and D. P. Shoemaker, *Acta Cryst.,* 1967, **22**, 162.

7   M. Grimm, B. Kirste, and H. Kurreck, *Angew. Chem.,* 1986, **98**, 1095; *Angew. Chem. Int. Ed.,* 1986, **25**, 1097.

8   a) G. P. Baxter, C. H. Hickey, and W. C. Holmes, *J. Am. Chem. Soc.,* 1907, **29**, 127; b) G. P. Baxter, and M. R. Grose, *J. Am. Chem. Soc.*, 1915, **37**, 1061.

9   D. F. Sava, K. W. Chapman, M. A. Rodriguez, J. A. Greathouse, P. S. Crozier, H. Zhao, P. J. Chupas, and T. M. Nenoff, *Chem. Mater.*, 2013, **25**, 2591.

10   H. Kitagawa, H. Ohtsu, and M. Kawano, *Angew. Chem. Int. Ed.*, 2013, **52**, 12395.

11   Z. Yin, Q. Wang, and M. Zeng, *J. Am. Chem. Soc.,* 2012, **134**, 4857.

12   Z. Zhang, W. Shi, Z. Niu, H. Li, B. Zhao, P. Cheng, D. Liao, and S. Yan, *Chem. Commun.*, 2011, **47**, 6425.

13   B. F. Abrahams, M. Moylan, S. D. Orchard, and R. Robson, *Angew. Chem. Int. Ed.*, 2003, **42**, 1848.

14   J. Y. Lu, and A. M. Babb, *Chem. Commun.*, 2003, 1346.

15   A. Funabiki, T. Mochida, K. Takahashi, H. Mori, T. Sakurai, H. Ohta, and M. Uruichi, *J. Mater. Chem.*, 2012, **22**, 8361.

16   T. Hasell, M. Schmidtmann, and A. I. Cooper, *J. Am. Chem. Soc.,* 2011, **133**, 14920.

17   M. Zeng, Q. Wang, Y. Tan, S. Hu, H. Zhao, L. Long, and M. Kurmoo, *J. Am. Chem. Soc.,* 2010, **132**, 2561.

18   Y. Wang, G. A. Sotzing, and R. A. Weiss, *Polymer*, 2006, **47**, 2728.

19   T. Hertzsch, F. Budde, E. Weber, and J. Hulliger, *Angew. Chem. Int. Ed.*, 2002, **41**, 2281.

20   C. H. Görbitz, M. Nilsen, K. Szeto, and L. W. Tangen, *Chem. Commun.*, 2005, 4288.

21   Z. Wang, Y. Zhang, T. Liu, M. Kurmoo, and S. Gao, *Adv. Funct. Mater.*, 2007, **17**, 1523.

22   J. Lang, Q. Xu, R. Yuan, and B. F. Abrahams, *Angew. Chem. Int. Ed.*, 2004, **43**, 4741.

23   a) P. H. Svensson, and L. Kloo, *Chem. Rev.*, 2003, **103**, 1649; b) P. Deplano, F. A. Devillanova, J. R. Ferraro, M. L. Mercuri, V. Lippolis, and E. F. Trogu, *Appl. Spectrosc.*, 1994, **48**, 1236.

24   A. J. Blake, F. A. Devillanova, R. O. Gould, W. Li, V. Lippolis, S. Parsons, C. Radek, and M. Schröder, *Chem. Soc. Rev.,* 1998, **27**, 195.

25   a) M. Kawano, M. Fujita, *Coord. Chem. Rev.,* 2007, **251**, 2592; b) Q. Chen, M. Zeng, L. Wei, M. Kurmoo, *Chem. Mater.,* 2010, **22**, 4328.

26   P. H. Svensson, M. Gorlov, and L. Kloo, *Inorg. Chem.,* 2008, **47**, 11464.

27   N. N. Greenwood, A. Earnshaw, *Chemistry of the Elements (2nd ed.)*, Butterworth-Heinemann, ISBN 0080379419, 1997.

28   A. Name, B. Name and C. Name, *Journal Title*, 2000, **35**, 3523; A. Name, B. Name and C. Name, *Journal Title*, 2000, **35**, 3523.
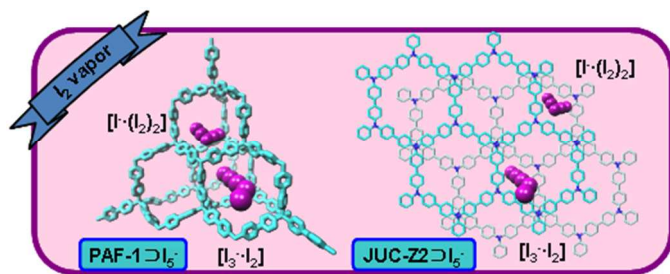
Porous organic frameworks such as PAF-1 and JUC-Z2 exhibits ultrahigh iodine adsorption.